Bulletin of Engineering Geology and the Environment (2019) 78:4673–4688
https://doi.org/10.1007/s10064-019-01465-7

ORIGINAL PAPER

Evaluation of the impact of karst depression-type impoundments on the underlying karst water systems in the Gejiu mining district, southern Yunnan, China

Hai-Yan Gao[1] · Ze-Min Xu[1] · Kun Wang[1] · Zhe Ren[1] · Kui Yang[1] · Yong-Jun Tang[1] · Lin Tian[1] · Ji-Pu Chen[1]

Received: 14 March 2018 / Accepted: 7 January 2019 / Published online: 4 February 2019

Abstract

The influence of mining activities on groundwater quality is a growing concern due to highly toxic metals in the tailings. Carbonate rocks are common in the surrounding rocks of ore deposits. But such mining districts generally do not have the conditions to construct traditional tailings impoundments due to the different degrees of karstification. This paper utilises field investigations, chemical analyses, and permeability tests, etc. to study the effect of tailings impoundments on the underlying karst water systems in the Gejiu world-class Sn-polymetallic mine located in a typical karst region in southern China, with samples collected from both karst springs deriving from the mining area and tailings porewater. Because of the abundance of sulphide minerals in the ores, acid mine drainage is expected to pose a high risk. However, the results indicate that the tailings porewater is moderately neutral and is characterized by the SO4–Ca–Mg hydrochemical type. This can be attributed to the substantial buffering capacity of carbonate minerals. Pollution elements in the tailings porewater mainly include SO_4^{2-} and toxic metals including As, Cd, Mn, Pb, and Hg. The type of pollution factors and the degree of contamination are not consistent in the different tailings impoundments. The hydrochemical classification of four karst springs distributed in the south of the mining area is HCO_3–Ca–Mg. The concentrations of SO_4^{2-} and the toxic constituents in the springs are far below the national standards for drinking water. The spring water not being contaminated may be attributed to the operation mode of the tailings impoundments (peripheral discharge and reuse of ponded water), the residual clay between the tailings impoundments and the carbonate bedrocks and the sufficient buffering capacity of the underlying karst systems. The tailings disposal at the Gejiu tin mine within the natural karst depressions is able to provide a reference for the operation of karst mines in China and elsewhere.

Keywords Tailings impoundment · Carbonate rock · Karst aquifer · Water quality assessment · Lateritic clay

Introduction

Mining operations produce large amounts of mine tailings. Tailings are deposited in impoundments in the vicinities of mining areas and generally contain high concentrations of toxic heavy metals (Ye et al. 2016). The annual accumulation of mine tailings in the world is over 10 billion tons (Wang et al. 2017). Such large quantities of mine tailings pose a potential pollution hazard to groundwater resources, because high concentrations of metals and metalloids can be discharged from mine wastes (Kusimi and Kusimi 2012; Brindha and Elango 2014; González-Fernández et al. 2017). Water contamination constitutes a threat on the natural ecosystems which support human health, biodiversity and food production. Hence, it is highly important to investigate groundwater quality in mining areas.

Increased knowledge of groundwater quality affected by mining operations could lead to sustainable utilization and effective management of water resources. There have been numerous studies on water hydrogeochemistry in mining areas around the world (Heikkinen et al. 2002; Dhakate et al. 2008; Amari et al. 2014; Acheampong and Nukpezah 2016). Quispe et al. (2013) studied the geochemistry of porewater in the vadose zone in the tailings impoundments

Electronic supplementary material The online version of this article (https://doi.org/10.1007/s10064-019-01465-7) contains supplementary material, which is available to authorized users.

✉ Ze-Min Xu
xzm768@kmust.edu.cn

[1] Faculty of Civil Engineering and Mechanics, Kunming University of Science and Technology, Kunming 650500, China

in the Iberian pyrite belt (SW Spain) which contain abundant sulphides yet lack carbonate to help buffer the acidification of its water by sulphides. The results showed that the porewater becomes heavily loaded with contaminants. Smuda et al. (2014) reported the temporal change of the porewater quality in the vadose zone of a carbonate-poor copper tailings impoundment in Chuquicamata, Chile. The results showed that the porewater had low pH and was enriched in mobile elements after a 5-year exposure. Huang et al. (2016) studied the effect of the Bayan Obo ring-dike impoundment in China on the porewater in the underlying Quaternary unconsolidated sediments and found that the plumes of inorganic contaminants (Mn, NH_4^+, F^- and SO_4^{2-}) were possibly caused by the pond leakage. At the same time, many studies have also focused on the environmental impacts of acid mine drainage (AMD; Nieto et al. 2007; Lei et al. 2010; Sahoo et al. 2016). Yet, very few studies have focused on the neutral mine drainage (NMD; Frau et al. 2017), especially on evaluating the effect of mining activities on groundwater in karst regions that were characterized by a relatively high degree of porosity and heterogeneity (Sun et al. 2013).

Carbonate rocks commonly surround ore deposits (Johnson et al. 2016). The widespread presence of highly karstic carbonate rocks on the surface and subsurface is one of the major features in karst areas. There is generally no suitable terrain to construct valley-type or ring-dike impoundments in these regions, and using karst depressions to contain tailings or constructing a certain height of low dams at the outlets of depressions to form larger scale tailings impoundments are the few options available. Because of the widespread distribution of karst depressions, such tailings impoundments are often constructed near mill sites to avoid high costs of transporting tailing slurries, while allowing the re-use of scarce water. The advantage of the tailings impoundments constructed in karst depressions is obvious, but there are unknown adverse environmental effects. Tailings impoundment seepage into underlying karst water is the main potential risk for karst depression-type impoundments compared to salt pan and in-pit impoundments.

The Gejiu tin mine is a world-class Sn-polymetallic mining area hosted in carbonate rocks which exploits different complex massive sulphide ores to obtain tin, copper, and lead concentrates. So far, it has operated for more than 200 years. Over 19 million tons of tailings (Gan 2009) are stored in more than 30 (active and inactive) karst depression-type impoundments. The rocks outcropped in the mining area are mainly limestone and dolomite. There is no surface water and the underlying karst water deriving from the mining area mostly drains into the Red River (Fig. 1).

Karst aquifers are extremely vulnerable environmental systems. Pollutants can often directly and easily enter the karst groundwater systems through sinkholes, dolines and fissures (Zhang et al. 2017). Nevertheless, because of the lack of suitable valleys for the construction of traditional tailings impoundments, the natural karst depressions are used for storing slurry tailings in the Gejiu mining area. Thus, the leakage from the mine tailings ponds into the karst systems can pose a potential threat to the valuable karst spring.

Fig. 1 Map showing the locations of the study area and sampling sites. (a) Yunnan province. (b) Surface water systems surrounding the study area. (c) Location of the tailings impoundments (red frames) and karst springs (magenta frames). The topographic map in Fig. 1c is based on SRTM 4.1 elevation data

Before this work, Zheng et al. (2009) gave an assessment on heavy-metal pollution in the Gejiu tin mine wasteland area. Their results indicated that the abundance of heavy metals was in the following order: Cd > Mn > Pb > As > Zn > Cu = Fe. The pollution levels of Cd, Mn, Pb and Zn were at least moderate, and the pollution levels of Cd and Mn were between intense and very intense, while the concentrations of Cu and Fe were extremely low. Kang and Yang (2017) performed a hydrogeological investigation at the Gaosong mine in the Gejiu tin mine and found that HCO_3^-, SO_4^{2-}, Na^+ and Ca^{2+} were the most abundant ions in the groundwater, and most of the groundwater with high SO_4^{2-} was slightly alkaline due to human activity.

However, there has been little focus on the effect of tailings on the karst spring water in the Gejiu mine so far. The aim of this paper is to evaluate the water quality of the springs to discuss whether they have been polluted by the tailings wastewater. This can also determine whether or not it is suitable to use natural karst depressions to construct tailings impoundments in the Gejiu mining area.

Site description

The Gejiu tin mine is located in Yunnan province, southwest China (Fig. 1a) and lies between north latitude 23°01′ to 23°36′ and east longitude 102°54′ to 103°25′, occupying a total area of about 1700 km^2. The mining district is situated in a karst mountain area and the elevations range from 1500 m to 2740 m a.s.l..

The Red River and Nanpan River are the major rivers controlling the drainage pattern of the area. The Red River flows from northwest to southeast and is an important international river located along the southern boundary of the study area (Fig. 1), with a total drainage area of approximately 138,748 km^2. The average annual flow rate is estimated to be 450 m^3/s. The research area has a typical subtropical monsoon climate with a mean annual temperature of 11.8 °C, ranging from −4.4 °C in winter to 35.6 °C in summer. The mean annual precipitation in this region is 1613 mm and approximately 85% of precipitation is concentrated in the rainy season from May to October (Li 2011). The mean annual evaporation is about 1203 mm (Peng and Li 2014).

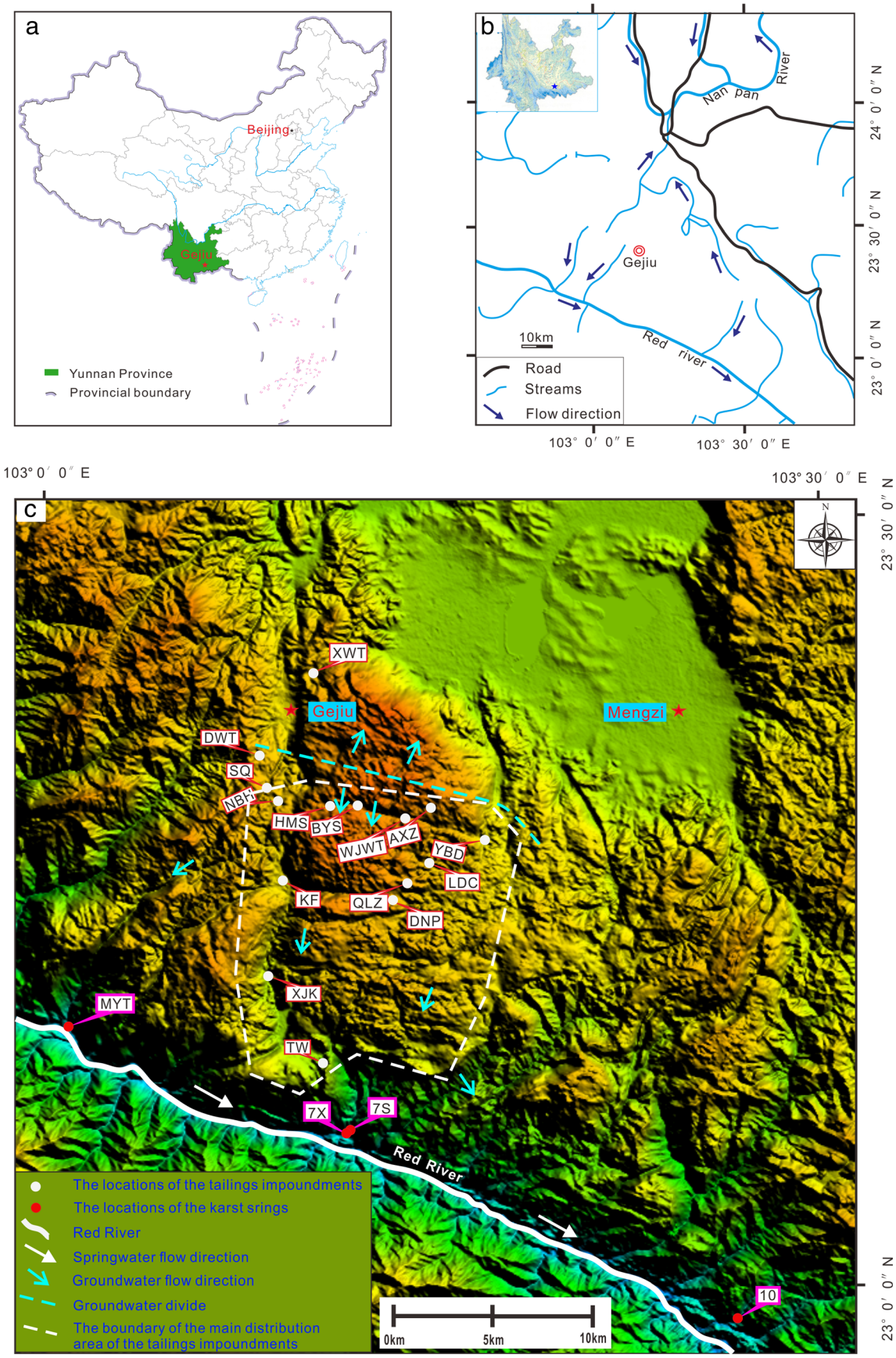
a
Beijing
Geju
Yunnan Province
Provincial boundary
b
Nan pan River
Geju
10km
Red river
Road
Streams
Flow direction
24° 0′ 0″ N
23° 30′ 0″ N
23° 0′ 0″ N
103° 0′ 0″ E
103° 30′ 0″ E
c
103° 0′ 0″ E
103° 30′ 0″ E
23° 30′ 0″ N
23° 0′ 0″ N
N
XWT
Geju
Mengzi
DWT
SQ
NBH
HMS
BYS
WJWT
AXZ
YBD
LDC
KF
QLZ
DNP
XJK
MYT
TW
7X
7S
10
Red River
The locations of the tailings impoundments
The locations of the karst srings
Red River
Springwater flow direction
Groundwater flow direction
Groundwater divide
The boundary of the main distribution area of the tailings impoundments
0km
5km
10km

The geology of the study area is complicated. Lithologically, the rocks outcropped in the mining area are mainly the carbonates of the middle Triassic Gejiu Group. The exploited ore consists of cassiterite-polymetallic sulphides and cassiterite-oxides, which are hosted by carbonate rocks, such as limestone and dolomite (Ni 2005; Gan 2009). Specifically, the mineral paragenesis consists of:

a) Cassiterite-polymetallic sulphides, of which pyrite and pyrrhotite are the main metallic minerals, and chalcopyrite, cassiterite, scheelite, bismuthinite, siderite, galena, arsenopyrite, and molybdenite are the minor metallic minerals. Calcite, quartz, fluorite, diopside, garnet, hornblende, and tremolite are the main gangue minerals.
b) Cassiterite-oxides, with limonite being the main ore, along with hematite and goethite. Cerusite, minetisite, plumbojarosite, cassiterite, and malachite occur as minor ore minerals, and calcite, quartz, sericite, clay, diopside, and garnet are the predominant gangue minerals.

After crushed and milled, the ore is treated by gravity separation, and flotation to separate minerals with high values (Zhao 2014). Chemical products used for the flotation are mainly lime which is used to adjust the pH between 10 and 12, as well as butyl xanthate and #2 oil as collectors and frothers, respectively. The tailings, in the form of slurry, are pumped into the tailings impoundments by the peripheral discharge method. The majority of the clarified water recovered after the sedimentation process is recycled back to the concentrators. The grain size of the tailings ranges from 0.04–917 μm, with medium sand, fine sand, and silt fractions being most abundant. The surface layer of the tailings shows diverse colours, including red-brown, greyish yellow, cinerous, and grey-black (Pan et al. 2015).

The karst depressions have been commonly used to construct tailings impoundments. There are generally several meters to tens of meters of the residual clay mainly found at the bottom and lower wall of the depressions. If not being covered completely by clay, the slopes of the periphery of the depressions would be lined with the clay excavated from adjacent depressions to avoid the impounded tailings coming into direct contact with the karstified carbonate rocks. Therefore, the lateritic clay beneath the tailings is mostly residual and partly transported.

As a result of extensive large-scale exploitation over the centuries, a number of abandoned and operating tailings impoundments have been formed in the study area. Figure 1 shows the main inactive and active tailings impoundments (TW, XJK, KF, SQ, NBH, HMS, BYS, WJWT, AXZ, YBD, LDC, QLZ, DNP, DWT, XWT). These sites were selected due mainly to their proximity to the mills. The storage capacity of these tailings impoundments ranges from 1.01 million m^3 to 32.4 million m^3 (Gan 2009).

The aquifer media is mainly composed of dolomitic and silty limestones (Lu 1985). The carbonate rocks in the mining district are highly karstified. The typical karst landscapes such as hills, depressions, trough valleys, sinkholes and dolines are widely distributed in the mining district. For example, there are 141 karst negative topographies within an area of about 27 km^2 near the WJWT tailings impoundment (Fig. 1c). Their average length, width and depth are 103 m, 60 m and 6.6 m, respectively, and the maximum length, width and depth are 873 m,

404 m and 69 m, respectively. Another important sign of strong karst development is that, although the annual rainfall is high, there is no natural surface water in the mining area, and 80% of the rainfall infiltrates into the subsurface through karst depressions, dolines, sinkholes, and fissures (Li 2011).

Karst water, which is the major type of groundwater in the mining area, is stored in karst channels and fissures, and is mainly derived from atmospheric rainfall. Besides the discharge of a small amount to Nan Pan River at the altitude from 1280 to 1379 m, most of the karst water in the mining area is discharged to the Red River in the form of karst springs at an altitude ranging from 250 to 336 m (Fig. 1). The main spring outlets are labelled as MYT, 7S, 7X and 10 (Fig. 1b, c). The flow rate of these karst springs is highly sensitive to rainfall. The springs MYT, 7X and 10 which are limpid in the dry season and turbid in the rainy season are perennial, and the flow rate in the rainy season is three to ten times that of the dry season. Spring 7S is seasonal and often turbid. Of the four springs, spring MYT and 7X are the sources of drinking water for the local residents and are also used for agricultural activities.

Sampling and analysis

Karst springs and tailings porewater were sampled in December 2016. The locations of the sampling sites were recorded with GPS and are shown in Fig. 1c. Karst spring samples (MYT, 7S, 7X, 10) were collected at the outlets of the springs. Tailings porewater samples from the tailings impoundments (TW, XJK, KF, SQ, NBH, HMS, BYS, WJWT, AXZ, YBD, LDC, QLZ, DNP, DWT, XWT) were collected from a certain depth below the dry beaches. In order to improve the reliability and reproducibility of the evaluation results, multiple sampling of the no. 7 (7S and 7X) karst springs, which are the major discharge points in the mining area, were carried out from December 2015 to December 2016 during both the wet and dry seasons. The 7S spring was sampled three times, in December 2015, July 2016 and December 2016. The 7X spring was sampled six times, in December 2015, and March, April, May, July and December 2016.

The water samples were collected in plastic polyethylene (PE) bottles pre-washed with diluted HCl and then rinsed three times with distilled water. Prior to sampling, these bottles were thoroughly rinsed again with water from the sampling site.

Physicochemical parameters including electrical conductivity (EC), pH, total dissolved solids (TDS) and water temperature of all the water samples were measured with a portable multi-parameter field meter three times consecutively to avoid errors in reading at the sampling sites. The samples were filtered through 0.45-μm regenerated cellulose then split into two sub-samples. One was acidified to pH < 2 with concentrated Suprapur HNO_3 in the field for cation and trace metal analysis. Another sample was for alkalinity and anion analyses and was left unacidified. All water samples were then sealed, transported to the laboratory and stored at 4 °C until further analysis.

Concentrations of dissolved Na, Mg, K, Ca, Cr, Mn, Fe, Co, Ni, Cu, Zn, As, Se, Mo, Ag, Cd, Ba, Hg, Pb, Sn, S, Si and Sb were determined by inductively coupled plasma mass spectrometry (ICP-MS; Agilent® 7700X). The detection limit for the analysed elements was about 0.006–22.25 μg/L. Analytical precision was better than ±5% depending on the concentration levels. Major cations (Na^+, K^+, Ca^{2+}, Mg^{2+} and NH_4^+) and anions (HCO_3^-, SO_4^{2-}, Cl^-, F^-, NO_2^-, and NO_3^-) were determined by ion chromatography (DIONEX® ICS2000). Alkalinity (as HCO_3^-) and H_2SiO_3 were analysed by titration with 0.1 M HCl and ultraviolet spectrophotometry, respectively. The reliability of the analysis results was checked by calculating the ion balance error.

Seven representative residual clay samples from two boreholes (ZK5 and ZK6, Fig. 2) were collected at different depths (ZK5#-1 at 15.00 m, ZK5#-2 at 16.40 m, ZK5#-3 at 18.21 m; ZK6#-1 at 15.30 m, ZK6#-2 at 16.85 m, ZK6#-3 at 18.10 m, ZK6#-4 at 19.77 m) from the surface to the layer of underlying clay subsoil in the WJWT tailings impoundment in March 2016.

The clay samples were packed in numbered and air-tight plastic bags and transported to the laboratory. After air-drying, grinding, sieving, and digesting, the contents of As, Hg, Co, Cd, Cr, Cu, Mo, Ni, Sn, Pb, Mn, and Zn in the samples were analysed. Permeability tests for the residual clay from the two boreholes were also performed.

Results

The analysis results of the tailings porewater, spring water, and residual clay are presented below.

Tailings porewater

The variations of the main hydrogeochemical parameters of tailings porewater are shown in Fig. 3. The boxplot used to represent the temporal concentration of the major parameters is a graphical mean for displaying the dispersion of the dataset. The boxplots of the tailings porewater samples show several outliers and extremes within the dataset, especially the SQ and XWT water samples.

The Piper diagram for the tailings porewater samples is shown in Fig. 4. Water samples are mainly SO_4^{2-}-Ca^{2+}-Mg^{2+} type and partly HCO_3^--Ca^{2+}-Mg^{2+} type. Measured pH values for tailings porewater are consistently near neutral. pH values vary slightly among the sites, with the highest value for AXZ (8.45) and the lowest value for TW (6.8).

Electrical conductivity (EC) is a measure of water capacity to convey electric current, and corresponds to the total dissolved solids (TDS; Prasanth et al. 2012). The EC of the tailings porewater samples ranges from 0.25 to 5.38 mS/cm (average 1.91 mS/cm). These values are attributed to high concentrations of Ca^{2+} and SO_4^{2-} along with other dissolved constituents (e.g., Mg^{2+}, Na^+, K^+, HCO_3^-) typically present in the tailings porewater. TDS in the tailings porewater varies from 150 (for QLZ) to 3805 mg/L (for XWT) with an average of 1515 mg/L, and exhibits a significant variation among the sampled impoundments. According to Sharma (2008), 50% of the tailings porewater samples can be classified as brackish water (TDS > 1000 mg/L).

The tailings porewater contains high SO_4^{2-}, Ca^{2+}, and elevated trace element (Mn, Cd, Pb, As) concentrations. Ca^{2+}, Mg^{2+}, Na^+, K^+, SO_4^{2-}, HCO_3^-, Cl^-, and F^- are the most abundant ions in the tailings porewater and contribute to the high TDS. Ca^{2+} is the most dominant cation. Mg^{2+} (1.72–193 mg/L) is the next dominant cation after Ca^{2+}. SO_4^{2-} is the dominant anion followed by HCO_3^-, Cl^-, and F^- in the tailings porewater. The SO_4^{2-} concentration ranges from 43.22 mg/L for AXZ to 2030.53 mg/L for XWT (average 926.02 mg/L) and varies widely across the region.

For trace elements, the tailings porewater is characterized by several elevated elements (Mn, As, Cd, Pb, Hg). Manganese concentration values change from 0.007 to 18.8 mg/L (average 3.44 mg/L). The highest concentration is found at site SQ, while the lowest value is at site QLZ. Arsenic analysis shows an abnormally high concentration of 0.335 mg/L at SQ, while the values at other sites range from 0.00188 to 0.10032 mg/L (average 0.04 mg/L). The Cd concentration is, on average, 0.06 mg/L with a standard deviation of 0.173 mg/L. The maximum value, 0.668 mg/L, is measured at site SQ. Pb and Hg concentrations vary from 0.00043 to 0.94001 mg/L, and 0.00027 to 0.00503 mg/L, respectively.

In short, the tailings porewater has poor water quality.

Karst spring

Constituent concentrations in the karst spring water compared to the national standards (NS) for drinking water (GB 5749-2006) are presented in Fig. 5. All the karst spring samples are colourless and odorless. The pH values vary from 7.07 to 8.06, with an average value of 7.36, indicating a range

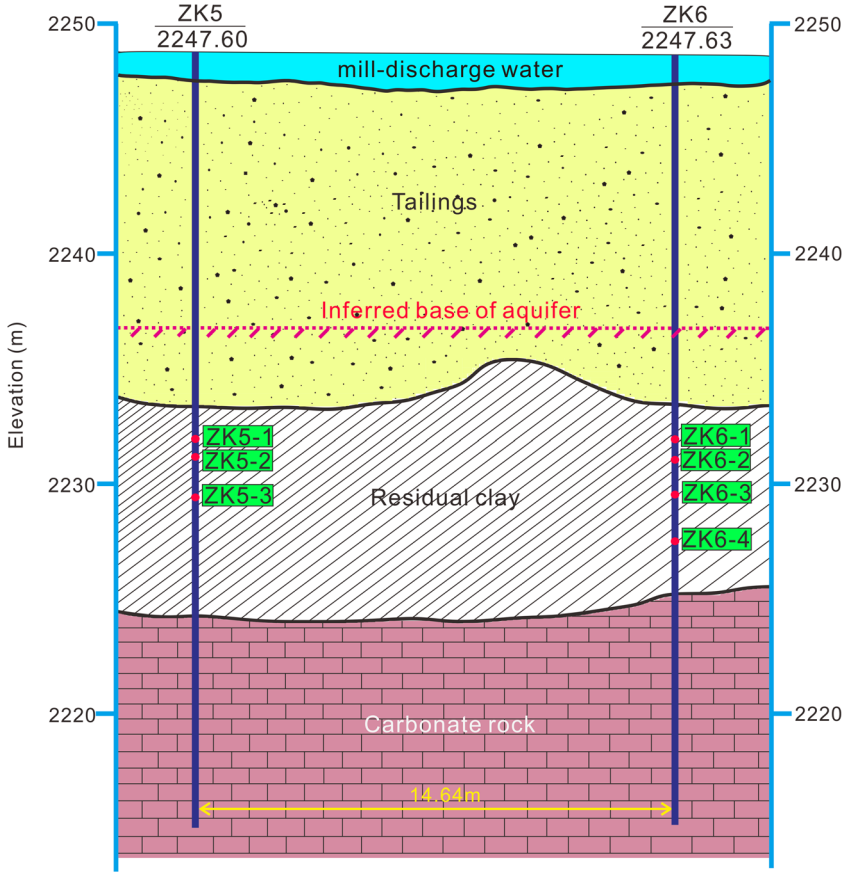

Fig. 2 Hydrogeological section of ZK5 and ZK6 in the WJWT tailings impoundment

of moderately neutral characteristics. The EC ranges from 0.245 to 0.488 mS/cm and the corresponding TDS ranges from 151 to 263 mg/L. All of the karst spring water samples can be classified as fresh water (0 < TDS < 1000 mg/L). The hardness (H_T) of the karst spring is calculated using the following equation (Pazand and Javanshir 2014):

$$H_T = 2.5Ca^{2+} + 4.1Mg^{2+}$$

The hardness values in karst spring samples range from 111.22 to 227.74 mg/l, with a mean of 197.94 mg/l. According to Pazand and Hezarkhani classification (2012), all of the water samples are hard. This is in accordance with the general characteristics of the groundwater in the karst region (Berhe et al. 2017; Fadili et al. 2016).

Among the major ions, the concentrations of HCO_3^-, SO_4^{2-}, Ca^{2+}, Na^+, and Mg^{2+} range from 136.3 to 260.4, 22.35 to 71.79, 34.78 to 79.45, 4.22 to 11.96, and 5.92 to 9.51 mg/L, respectively. Additionally, the heavy-metal pollution is of greater concern than the acidity in terms of environmental damage (Idaszkin et al. 2017). The heavy metals have concentrations of: Mn (2.96–11.1 μg/l), As (1.55–4.43 μg/l), Cr (0.45–0.68 μg/l), Co (0.06–0.07 μg/l), Fe (0.04–0.11 mg/l), Cd (0.04–0.11 μg/l), Cu (1.07–5.81 μg/l), Pb (0.84–4.32 μg/l), and Hg (0.13–0.42 μg/l) among the karst spring water samples (Figs. 5 and 7). The statistical parameters in the karst spring compared with the NS for drinking water indicate that they are all below the standard values of the NS for drinking water (Fig. 5) and are suitable for drinking.

Hydrochemical classification using the Piper diagram (Fig. 4) showed that only one spring water type is present, HCO_3–Ca–Mg, which is a typical type of karst water.

The results of the multiple sampling for metal elements from 7S and 7X are presented in Fig. 6. The concentrations of the metal elements show no significant seasonal variation. The concentrations of Mn are unusually high in July 2016 (7S) and May 2016 (7X). Nevertheless, it is still within the NS for drinking water (GB 5749-2006).

The Pearson's correlation coefficient matrix between major ions and physical parameters in the karst springs is shown in Table 1. The significant positive correlations between Mg^{2+}, Ca^{2+}, and HCO_3^- are found, but there are weak correlations between Mg^{2+}, Ca^{2+}, and SO_4^{2-}. Likewise, there are also moderately positive correlations between Fe and Mn (Fig. 7a), but no significant correlations between Cu and Ba, Pb and Ba, and As and Mn (Fig. 7 b, c, d).

Residual lateritic clay

The concentrations of metal elements in the residual lateritic clay are summarized in Table 2. All residual clay samples are

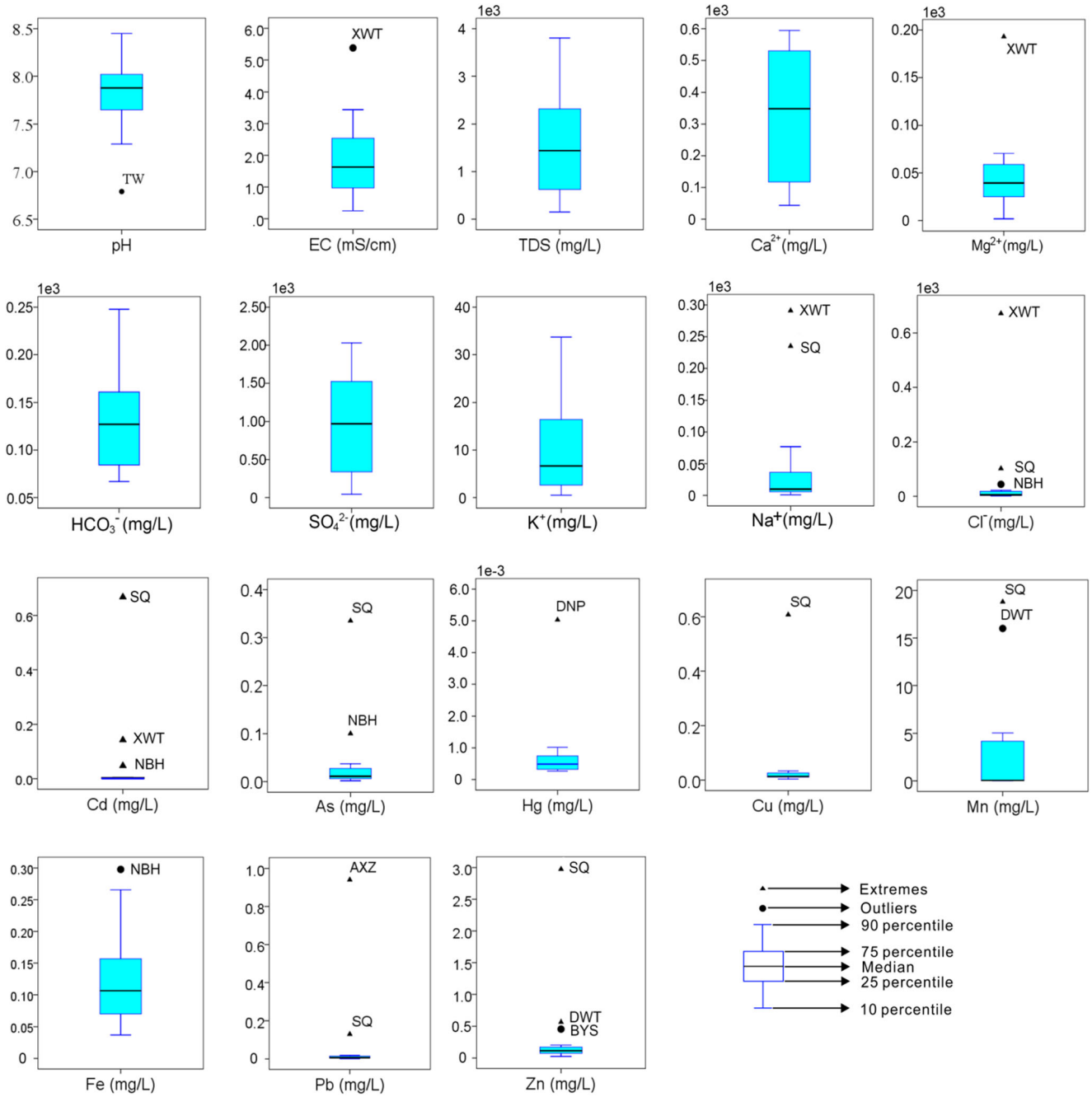

Fig. 3 Box plots of the main hydrogeochemical parameters of the tailings porewater

characterized by moderately neutral pH. The mean concentrations of metal elements are greater than the grade II environmental quality standard for soils (GB 15618-2008). The mean concentrations follow the order: Mn > Pb > Zn > Ni > Cr > Cu > As > Co > Mo > Sn > Cd > Hg.

The mean permeability coefficients of the residual clay samples collected from the two boreholes shown in Fig. 2 are 6.9×10^{-7} cm/s and 1.2×10^{-7} cm/s, respectively. The maximum particle diameters of the clay samples are between 2 and 5 mm, and the cumulative percentages of the fractions <0.075 mm are all greater than 95%.

Discussion

Hydrochemical characteristics of major ions

The Piper diagram shows significant differences between the tailings porewater and the karst spring water (Fig. 4). The karst spring water is characterized by HCO_3–Ca–Mg type, which is typical in karst regions (Pu et al. 2013). On the contrary, the tailings porewater is characterized by SO_4–Ca–Mg type. The different hydrochemical compositions of the waters reflect different hydrogeochemical processes.

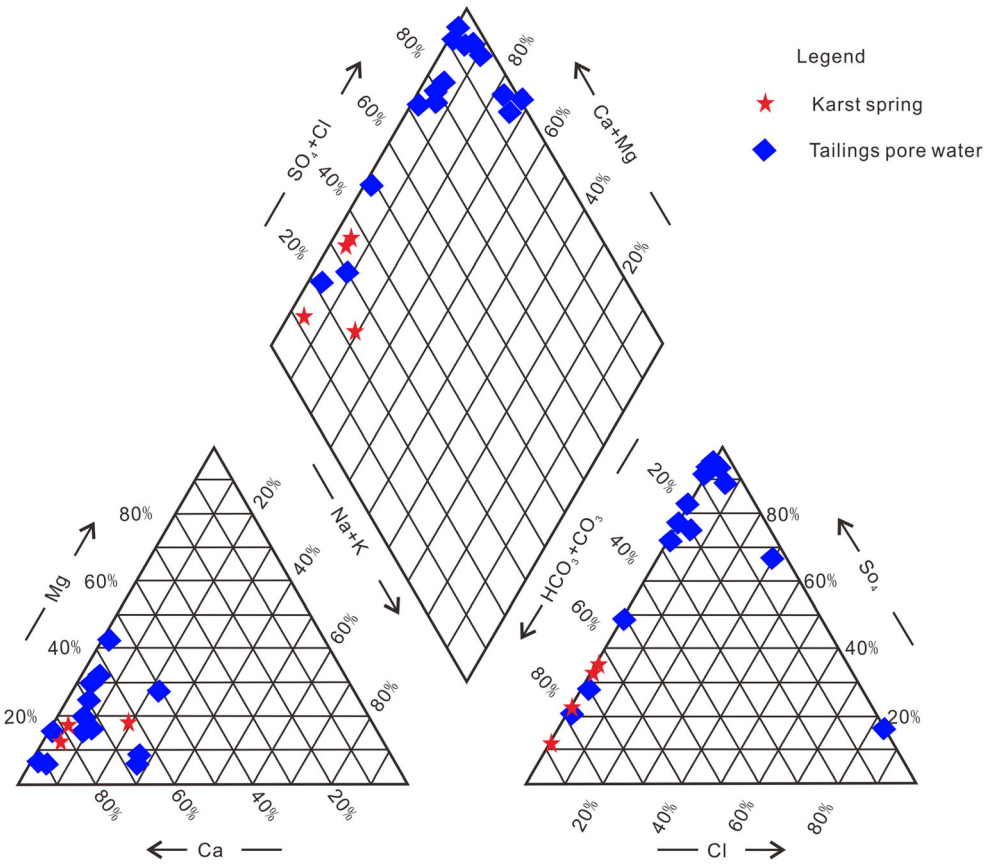

Fig. 4 Piper diagram of all of the water samples

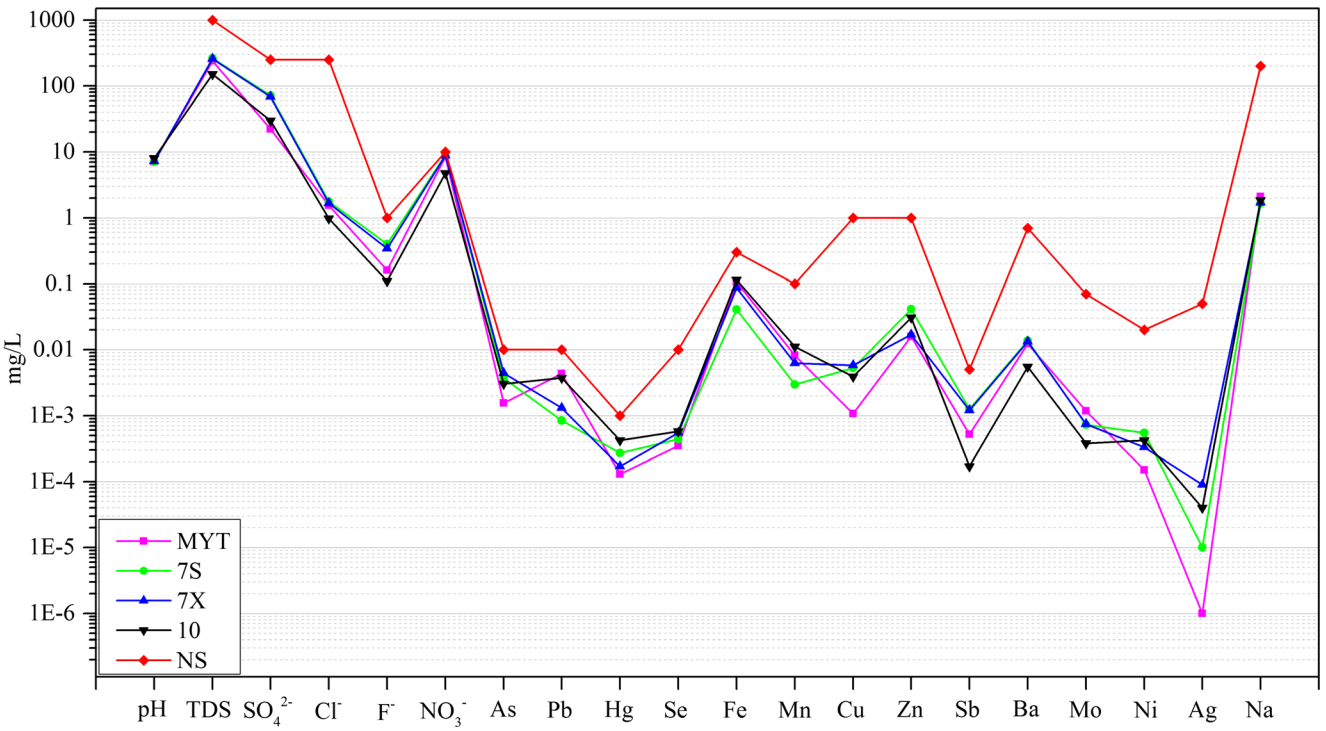

Fig. 5 Constituent concentrations of various elements and ions in the karst spring water compared to the national standards (NS) for drinking water (GB 5749-2006)

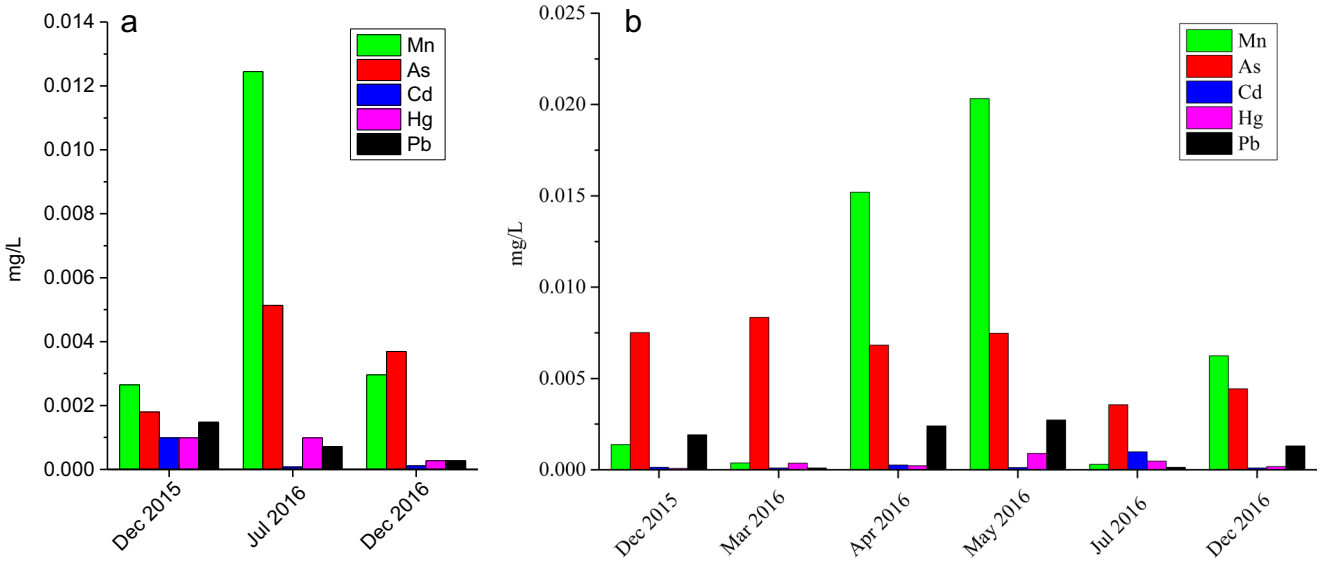

Fig. 6 Concentrations of the main elements from multiple sampling of sites 7S (a) and 7X (b)

It is known that when sulphide minerals, such as pyrite, pyrrhotite, galena (PbS), and sphalerite (ZnS) which have been shown to be abundant in the tailings deposits (Zhuang et al. 1996), are exposed to oxygen and moisture, they will easily oxidize, thus produce SO_4^{2-} and acidic wastewater. The tailings porewater should theoretically be characterized by low pH. The process of pyrite and pyrrhotite oxidation is described by the reaction presented in Eqs. 1 and 2 (Gomo and Vermeulen 2014).

$$FeS_2 + 4.5O_2 + 3.5H_2O \rightarrow Fe(OH)_{3(s)} + 2SO_4^{2-} + 4H^+ \quad (1)$$

$$Fe_{1-x}S + \frac{9-3x}{4}O_2 + \frac{5-3x}{2}H_2O \rightarrow (1-x)\,Fe(OH)_{3(S)} + SO_4^{2-} + 2H^+ \quad (2)$$

However, the analysis results seem to be contrary to the above expectations. High concentration of SO_4^{2-} are present, but the pH values for the tailings porewater are moderately alkaline for all of the samples (Fig. 3). This is most possibly the result of buffering by the carbonate minerals, such as calcite and dolomite, on the acidic wastewater produced by the sulphide mineral oxidation, which explains the high concentrations of SO_4^{2-}, Ca^{2+}, and Mg^{2+}, together with the low HCO_3^- concentrations.

As stated above, calcite and dolomite widely occur in the ore bodies throughout the region. The acidic wastewater (Eqs. 1 and 2) is buffered by calcite and dolomite as described by the reactions shown in Eqs. 3 and 4 (Gomo and Vermeulen 2014).

$$2CaCO_3 + 4H^+ \rightarrow 2Ca^{2+} + 2H_2O + 2CO_2 \quad (3)$$

$$CaMg(CO_3)_2 + 4H^+ \rightarrow Ca^{2+} + Mg^{2+} + 2H_2O + 2CO_2 \quad (4)$$

Correlations between dissolved species can determine the origin of solutes and the process that generates the water compositions (Sánchez et al. 2017). Figure 8 a–c gives scatter plots of SO_4^{2-} against Ca^{2+} and Mg^{2+} concentrations in the tailings porewater samples. SO_4^{2-} is highly correlated to Ca^{2+} (Fig. 8a) and is moderately correlated to Mg^{2+} (Fig. 8b) with positive correlation coefficients of 0.98 and 0.64, respectively. The relationship between SO_4^{2-} and $Ca^{2+} + Mg^{2+}$ exhibits a linear positive relationship, with correlation coefficients of 0.99 (Fig. 8c). This shows that SO_4^{2-}, Ca^{2+}, and Mg^{2+} in the tailings porewater are controlled by the same geochemical process, and according to the mineral composition of the tailings, these processes should be Eqs. 1, 2, 3, and 4.

Only one water type (HCO_3–Ca–Mg) in the karst spring samples reflects the occurrence of similar hydrogeochemical processes as influenced by natural processes. The dominant ion compositions (Ca^{2+}, Mg^{2+}, HCO_3^-) imply the major reactants are carbonate rocks. The dissolution of calcite and dolomite in the karst aquifers yields Ca^{2+}, Mg^{2+}, and HCO_3^-, which can be described by the following equations.

$$CaMg(CO_3)_2 + 2H_2O + 2CO_2 \rightarrow Ca^{2+} + Mg^{2+} + 4HCO_3^- \quad (5)$$

$$CaCO_3 + CO_2 + H_2O \rightarrow Ca^{2+} + 2HCO_3^- \quad (6)$$

The dissolution of calcite and dolomite (Eqs. 5 and 6) determines the ratios of dissolved ions. If the water is formed by single dissolution of calcite, the ratio of bicarbonate to calcium will be 2:1, whereas if it is from dissolution of dolomite, the ratio will be 4:1 (Liu et al. 2017). Figure 8(d) shows the scatter plot for the two ions. The karst spring lies in a transition region where calcite and dolomite will both dissolve. In addition, Table 1 shows significant positive correlations between Ca^{2+}, Mg^{2+}, and HCO_3^-, which also suggests the dissolution of calcite and dolomite. The karst spring also contains NO_3^-, most

Table 1 Pearson correlation coefficients among the major ions and physical parameters in the karst spring water samples

	pH	TDS	EC	Ca^{2+}	Mg^{2+}	Na^{+}	HCO_3^-	SO_4^{2-}
pH	1							
TDS	−0.962*	1						
EC	−0.989*	0.972*	1					
Ca^{2+}	−0.978*	0.995**	0.991**	1				
Mg^{2+}	−0.700	0.493	0.676	0.575	1			
Na^{+}	0.991**	−0.970*	−1.000**	−0.990*	−0.687	1		
HCO_3^-	−0.859	0.702	0.844	0.768	0.966**	−0.852	1	
SO_4^{2-}	−0.425	0.645	0.454	0.567	−0.346	−0.442	−0.091	1

** Correlation is significant at the 0.01 level

* Correlation is significant at the 0.05 level

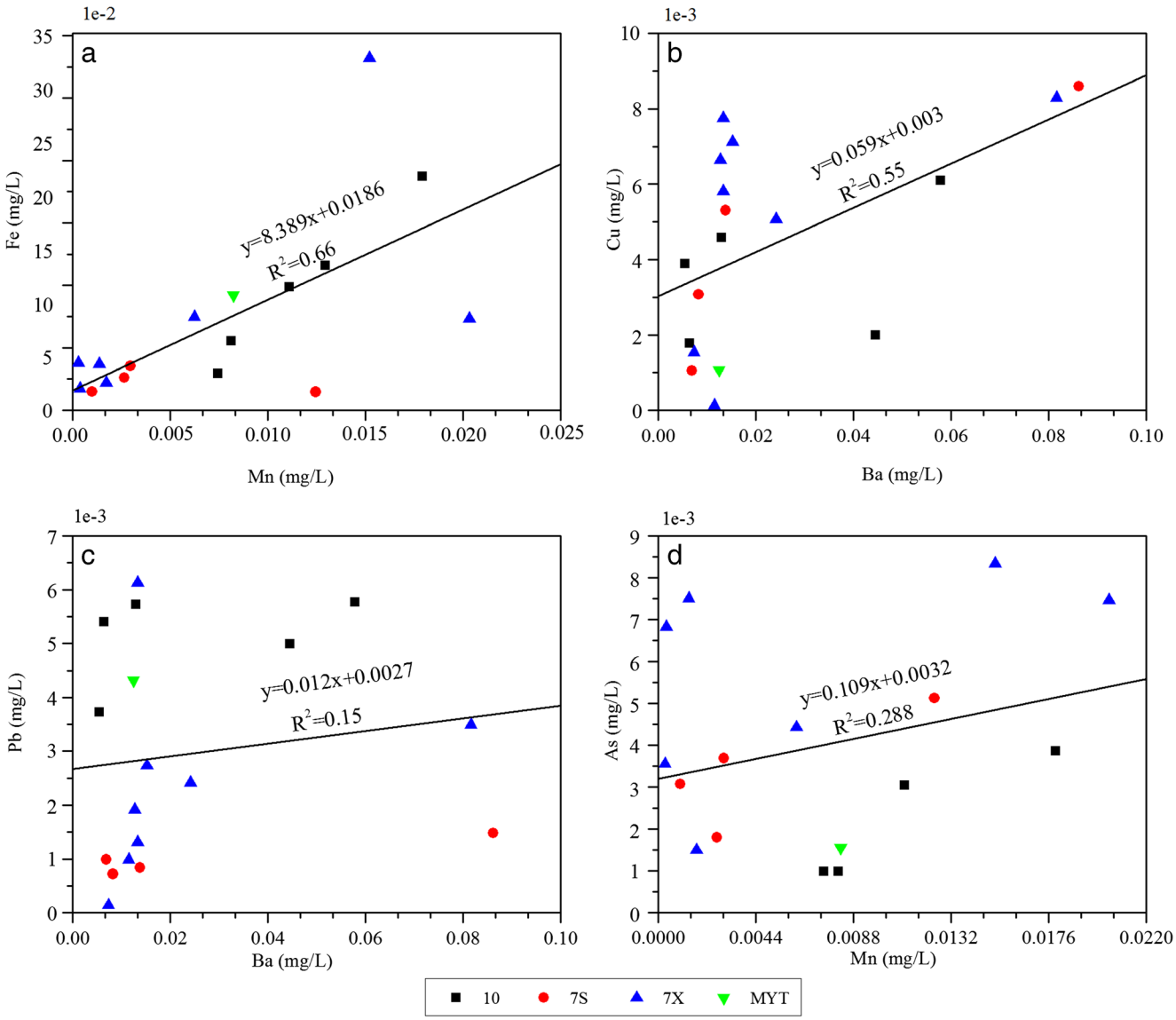

Fig. 7 Scatterplots of relationships between selected variables for the karst spring water samples: (a) Fe vs. Mn; (b) Cu vs. Ba; (c) Pb vs. Ba; (d) As vs. Mn

Table 2 Analysis results of selected metal elements in the residual clay. All values are in mg/kg, except for pH

Sample	pH	As	Hg	Co	Cd	Cr	Cu	Mn	Mo	Ni	Pb	Sn	Zn
ZK5–1	7.45	95.9	1.21	51.4	3.34	242	120	3400	13	106	750	11.9	990
ZK5–2	7.96	111	1.3	62	3.06	252	108	4800	12.9	145	820	11.3	1000
ZK5–3	7.85	68.5	1.8	57.2	2.71	236	124	9300	12	231	1100	7.49	1300
ZK6–1	7.66	89.2	0.27	56.2	1.55	186	118	5000	7.74	91.1	740	8.41	750
ZK6–2	7.64	108	1.28	43.8	2.57	274	146	6000	10.7	165	1100	9.25	950
ZK6–3	7.47	55.3	2.39	58.4	2.94	237	148	14,200	19.3	456	1600	7.69	1400
ZK6–4	7.46	64.3	3.09	65.1	3.01	261	162	16,800	19.4	600	2000	6.69	1500
mean	7.64	84.6	1.62	56.3	2.74	241	132	8500	13.6	256	1158	8.96	1127

possibly originating from leaching of chemical fertilizers and animal manure, septic tank effluents, and domestic sewage discharges throughout the region.

The foregoing analysis shows that the solutes of the tailings porewater and the karst spring water are derived from the different hydrogeochemical processes. In addition, the levels of the constituents in the karst spring water are far below those of the tailings porewater (Figs. 3, 7, and 9). To a certain degree, it is shown that the tailings water does not leak into the karst spring.

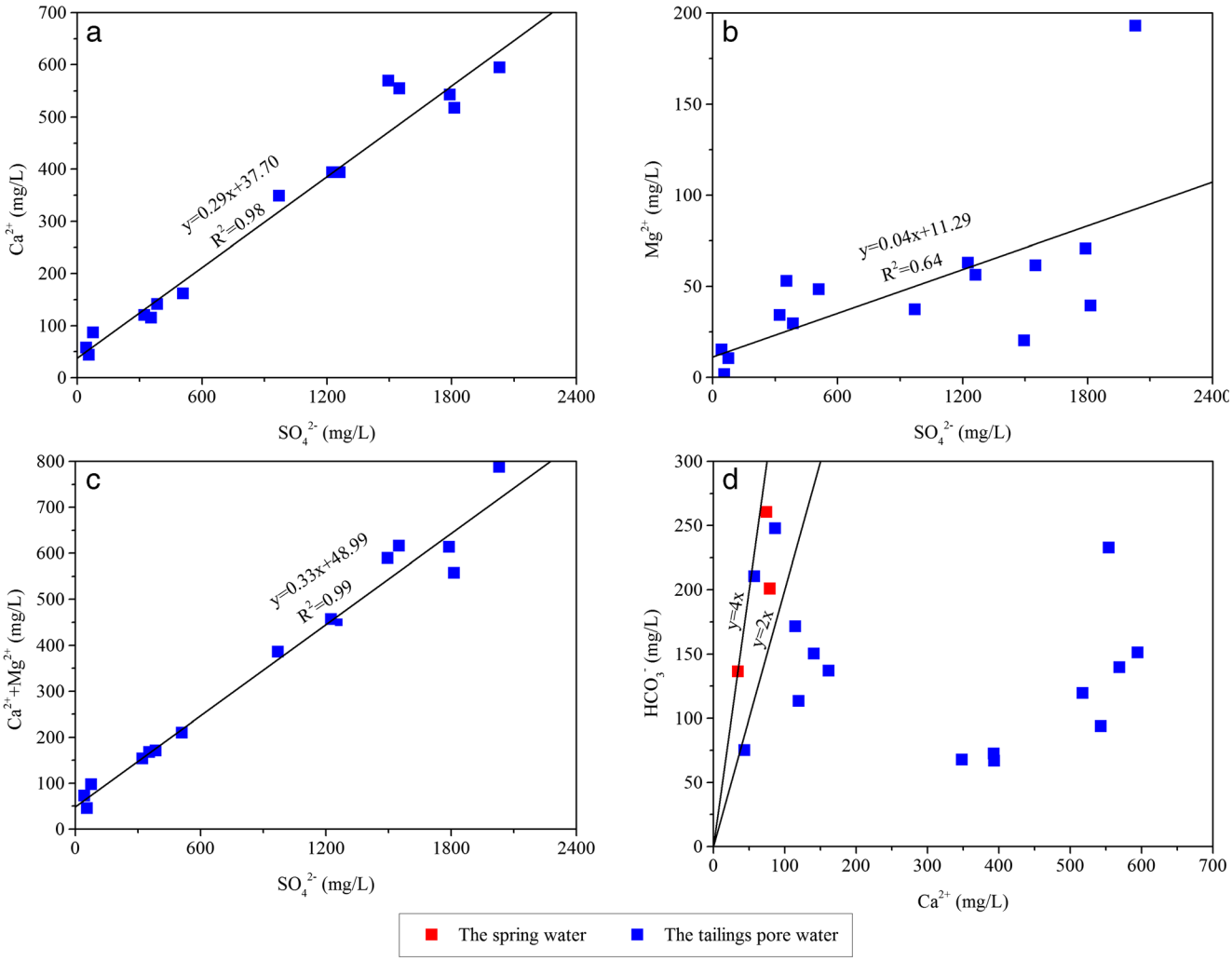

Fig. 8 Relationships between dissolved ions in the water: (a) SO_4^{2-} vs. Ca^{2+}, (b) SO_4^{2-} vs. Mg^{2+}, (c) SO_4^{2-} vs. the sum of Ca^{2+} and Mg^{2+}, (d) Ca^{2+} vs. HCO_3^-

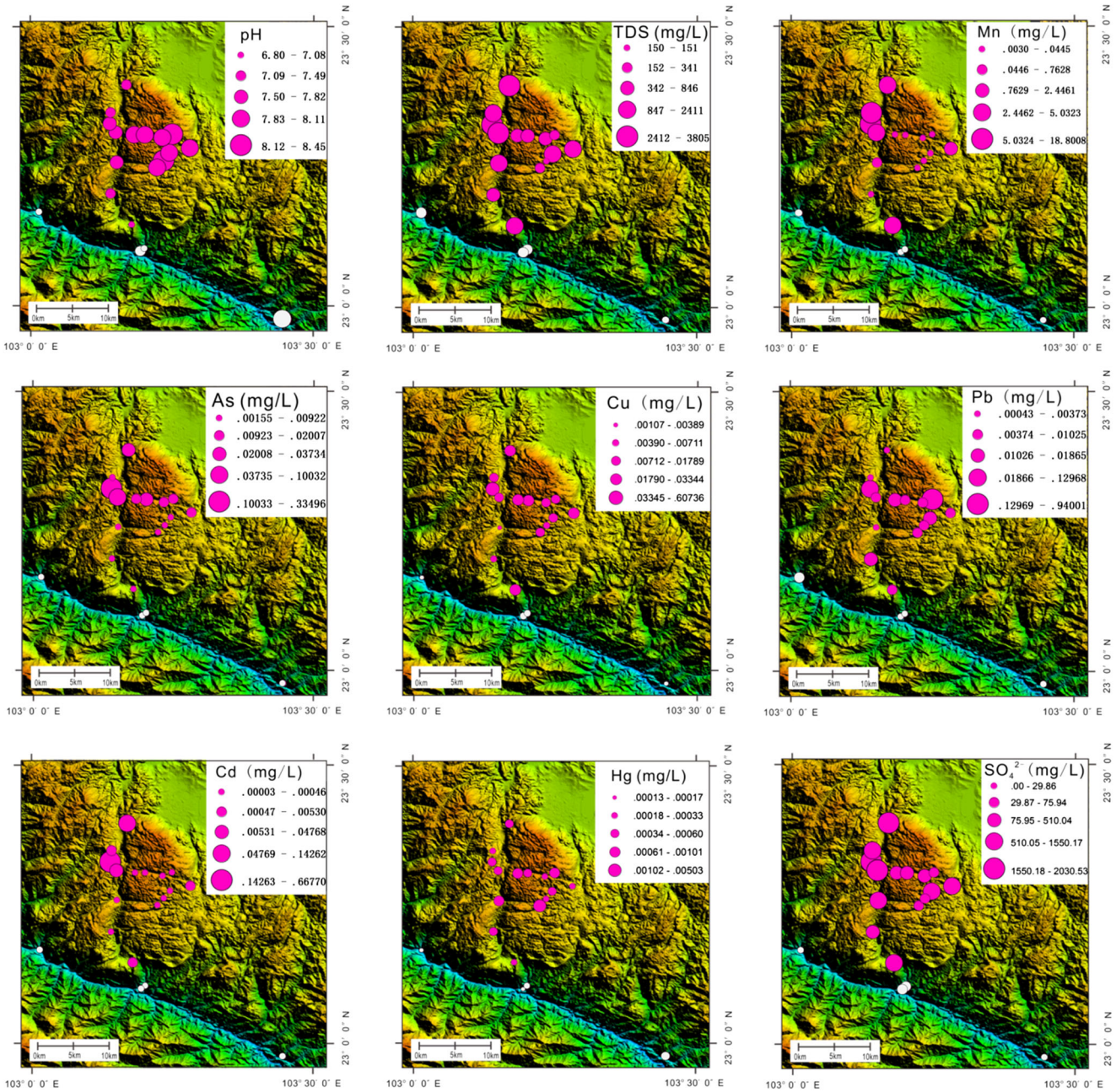

Fig. 9 Spatial distribution of selected pollution indicators (pH, TDS, Mn, As, Cu, Pb, Cd, Hg, SO_4^{2-}). The topographic maps were compiled with SRTM4.1 data

Geochemical factors preventing pollution

The operation mode of tailings impoundments

As described above, at the Gejiu mine sites, the flotation tailings are typically in the form of slurries whose water content is high and viscosity is low. The tailings are pumped into the tailings impoundments through peripheral discharge. This disposal technique causes hydraulic sorting of the tailings particles, and results in the formation of a beach with coarsening grain size from the centre toward the perimeter of the impoundment. As a result of this variable gradation, the mill discharge water does not immediately infiltrate into the tailings but runs off toward the centre of the impoundment, forming a pond as shown in Fig. 10 (Al and Blowes 1999). The pond can be maintained for several months due to high compaction and low permeability of the underlying tailings (Triantafyllidis et al. 2007). The clarified water in the pond is decanted and pumped to the mill for reuse. Hence, seepage through tailings impoundment is nearly zero.

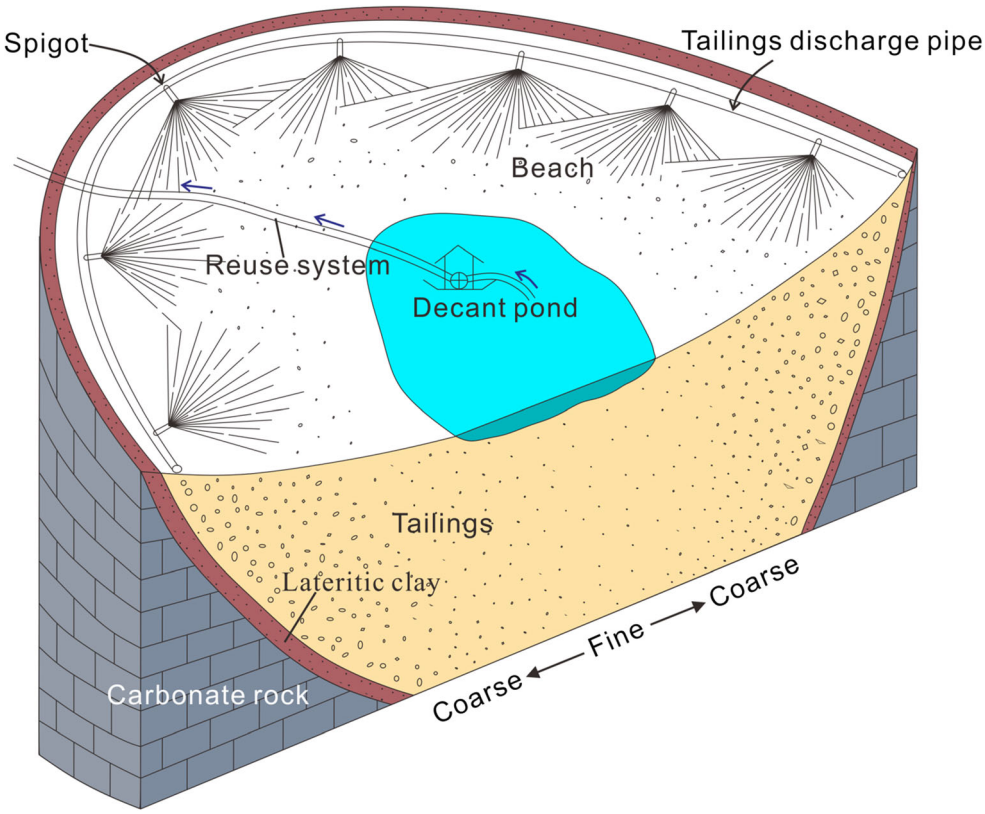

Fig. 10 Schematic diagram showing the peripheral discharge of tailings slurries used in the Gejiu mining district

Low permeability of the tailings

Because of the fine-grained nature, tailings material has commonly low permeability (Wickland and Wilson 2005; Sözen et al. 2017) and can be an impervious barrier under the loading of further tailings deposits.

The mean permeability coefficient of the six tailings samples collected from the WJWT tailings impoundment is 2.38×10^{-6} cm/s with standard deviation of 3.86×10^{-6} cm/s. There are two ponds in the AXZ tailings impoundment, which are about 10 m apart from each other and the height difference of the water level is 6 m (Fig. 11), suggesting that there is little connectivity between the two ponds and low permeability of the tailings deposit.

Impermeability and adsorption capacity of the residual clay

Natural clay is largely responsible for the low hydraulic conductivity of earthen liners, which provides the most economical liners for tailings impoundment construction. Natural clay serves as hydraulic barriers to flow of fluids and are used to control release of leachate from the waste (Daniel 1993). The residual clay overlying the carbonate rocks in the Gejiu area is highly enriched, especially in the natural depressions. The thickness of clay varies from several meters to tens of meters. The clay with low permeability described above can serve as a barrier impervious to infiltration and movement of contaminants from the impoundments to the underlying karst systems.

Furthermore, the elevated concentrations of the elements in the residual clay are coincident with their high levels in the tailings porewater (Fig. 3 and Table 2). This indicates that the clay is an effective adsorbent for removing toxic heavy metals from aqueous solutions (Uddin 2017). pH is the most critical parameter that affects the adsorption process because it causes electrostatic changes. Zn and Pb can be adsorbed by the soil particles and can not migrate more deeply into the groundwater under neutral conditions (Kusimi and Kusimi 2012). This explains the low toxicity levels of Zn and Pb in the spring because the pH of the samples analysed was nearly neutral. The sediment samples with pH of 7.8–8.8 can promote the high adsorption of Zn and Cu and precipitation of Pb (Azhari et al. 2016). Obviously, this type of hydrogeochemical processes may also occur in the residual clay with pH of 7.45–7.96 in the study area. In general, clay particles are inclined to be enriched in trace elements (Wang et al. 2018). Therefore, the residual clay with a cumulative 95% of particles <0.075 mm in the study area has excellent adsorption capacity. Furthermore, under neutral conditions, the dissolved metals and metalloids in solution may precipitate or co-precipitate with hydroxides or in carbonates such as ferrihydrite, siderite, and cerussite. In such cases, they can be efficiently immobilized in the solid phase, and can't be transported by flowing water (Nejeschlebová et al. 2015).

Fig. 11 Two adjacent ponds with different water tables within the AXZ tailings impoundment

Environmental capacity of the karst system

The tailings and clay barriers physically restrict the quantity of seepage and reduce the concentrations of contaminants in the leachate. The quantity of seepage through the foregoing two barrier layers should be very small and this seepage impact can be further mitigated by the interaction between the leachate and the karst systems.

The walls of the karst conduits react with the leachates, creating neutral solutions, which results in precipitation of the contaminants. In addition, the water in karst systems can provide self-purification in the form of dilution and diffusion of contaminants, and buffering the contaminants. For the scarce leachate infiltrating into the karst systems, the environmental capacity of the considerable unsaturated zone is obviously huge. The karst systems can be viewed as additional buffer zones between the impoundments and the discharge points or filters to remove undesirable substances (Nakhaei et al. 2015) before they affect the karst springs.

Therefore, the environmental capacity of the karst systems should be one of the contributors such that the contaminants in the tailings porewater cannot be detected in the karst springs.

In conclusion, the sorted tailings, the residual clay, and the karst systems form a combined leakage control system for the karst depression-type impoundments in the Gejiu mining district, which protects the karst water against pollution. However, considering the high karstification in the mining district, maintaining water quality monitoring for the karst springs is still necessary.

Conclusions

The Gejiu tin mine is the largest Sn-polymetallic mine hosted in carbonate rocks in the world. The mining region is characterized by extensive development of karstic features on the surface and underground and is dotted by more than 30 karst depression-type impoundments. This paper utilised field investigations, chemical analyses, and permeability tests, etc. to investigate the effect of the tailings impoundments on the underlying karst water. The main conclusions are as follows:

1) The Gejiu ore has an abundance of sulphide minerals and, therefore, there should be a high risk of acid mine drainage. However, analysis indicates that the tailings porewater is moderately neutral and characterized by SO_4–Ca–Mg hydrochemical type. This can be attributed to the substantial buffering capacity of the carbonate minerals in the tailings deposits.
2) Pollution elements identified in the tailings porewater mainly are SO_4^{2-} and toxic metals including As, Cd, Mn, Pb, and Hg. However, the type of pollution factors and the degree of contamination are not consistent in the different tailings impoundments. This is related to the history of tailings storage and the types of ores as the tailings sources.
3) The hydrochemical type of the four karst springs distributed in the south of the mining area is HCO_3–Ca–Mg type. The concentrations of SO_4^{2-} and the toxic constituents (As, Cd, Mn, Pb, and Hg) are very low and far below the national standards (NS) for drinking water.
4) The karst water has not been contaminated by the tailings impoundments in the Gejiu mine, and this may be attributed to the operation mode of the tailings impoundments (peripheral discharge and reuse of ponded water), the residual clay between the tailings impoundments and the carbonate bedrocks, and the sufficient environmental capacity of the underlying karst systems.
5) Carbonate rocks are important ore-bearing rocks, and it is often difficult to find suitable sites to construct the common valley-type impoundments in the mining areas with the extensive development of karstic features. The Gejiu

tin mine storing tailings with karst depressions provides a reference for the operation of karst mines in China and elsewhere by optimizing the operation mode of tailings discharge into the impoundments and fully utilizing residual clay as an impermeable and adsorptive barrier.

Acknowledgements This work is supported by the National Natural Science Foundation of China-Yunnan Joint Fund (U1502232, U1033601) and Research Fund for the Doctoral Program of Higher Education of China (20135314110005). We greatly appreciate the anonymous reviewers' pertinent comments on this work.

References

Acheampong EA, Nukpezah D (2016) Assessing the impact of an operating tailings storage facility on catchment surface and groundwater quality in the Ellembele District of the Western region of Ghana. Environ Pollut 5(2):26–40

Al TA, Blowes DW (1999) The hydrogeology of a tailings impoundment formed by central discharge of thickened tailings: implications for tailings management. J Contam Hydrol 38(4):489–505

Amari KE, Valera P, Hibti M, Pretti S, Marcello A, Essarraj S (2014) Impact of mine tailings on surrounding soils and ground water: case of Kettara old mine, Morocco. J Afr Earth Sci 100:437–449

Azhari AE, Rhoujjati A, Hachimi MLE (2016) Assessment of heavy metals and arsenic contamination in the sediments of the Moulouya River and the Hassan II dam downstream of the abandoned mine Zeïda (high Moulouya, Morocco). J Afr Earth Sci 119: 279–288

Berhe BA, Dokuz UE, Çelik M (2017) Assessment of hydrogeochemistry and environmental isotopes of surface and Groundwaters in the Kütahya plain, Turkey. J Afr Earth Sci 134:230–240

Brindha K, Elango L (2014) Geochemical modelling of the effects of a proposed uranium tailings pond on groundwater quality. Mine Water Environ 33(2):110–120

Daniel DE (1993) Clay liners. In: Daniel DE (ed) Geotechnical practice for waste disposal. Springer, Boston, MA, pp 137–163

Dhakate R, Singh VS, Hodlur GK (2008) Impact assessment of chromite mining on groundwater through simulation modeling study in Sukinda chromite mining area, Orissa, India. J Hazard Mater 160(2–3):535–547

Fadili A, Najib S, Mehdi K, Riss J, Makan A, Boutayeb K, Guessir H (2016) Hydrochemical features and mineralization processes in coastal groundwater of Oualidia, Morocco. J Afr Earth Sci 116: 233–247

Frau F, Pelo SD, Atzori R, Cidu R (2017) Impact on streams and sea water of a near-neutral drainage from a flooded mine in Sardinia, Italy. Proc Earth Planet Sci 17:213–216

Gan FW (2009) Research on material composition and contamination transmission of tailings in tin-polymetallic mine of Gejiu. Ph. D thesis, China University of Geosciences, Beijing (in Chinese)

GB 5749 (2006) Standards for drinking water quality. National Standardization Administration Committee of the Ministry of Health of the People's Republic of China, Beijing (in Chinese)

GB 15618 (2008) Soil environmental quality standard. General Administration of quality supervision, inspection and Quarantine of the Ministry of environmental protection (in Chinese)

Gomo M, Vermeulen D (2014) Hydrogeochemical characteristics of a flooded underground coal mine groundwater system. J Afr Earth Sci 92(4):68–75

González-Fernández B, Rodríguez-Valdés E, Boente C, Menéndez-Casares E, Fernández-Braña A, Gallego JR (2017) Long-term ongoing impact of arsenic contamination on the environmental compartments of a former mining-metallurgy area. Sci Total Environ 610-611:820

Heikkinen P, Korkka-Niemi K, Lahti M, Salonen VP (2002) Groundwater and surface water contamination in the area of the Hitura nickel mine, Western Finland. Environ Geol 42(4):313–329

Huang X, Deng H, Zheng C, Cao G (2016) Hydrogeochemical signatures and evolution of groundwater impacted by the Bayan Obo tailing pond in northwest China. Sci Total Environ 543(Pt A):357

Idaszkin YL, Mdp A, Carol E (2017) Geochemical processes controlling the distribution and concentration of metals in soils from a Patagonian (Argentina) salt marsh affected by mining residues. Sci Total Environ 596–597:230–235

Johnson AW, Gutiérrez M, Gouzie D, Rex McAliley L (2016) State of remediation and metal toxicity in the tri-state Mining District, USA. Chemosphere 144:1132–1141

Kang DM, Yang ZP (2017) The hydrogeological investigation in Gaosong field of Gejiu tin mine. Chin Min Mag 26(s1):191–194 (in Chinese)

Kusimi JM, Kusimi BA (2012) The hydrochemistry of water resources in selected mining communities in Tarkwa. J Geochem Explor 112(1): 252–261

Lei LQ, Song CA, Xie XL, Li YH, Wang F (2010) Acid mine drainage and heavy metal contamination in groundwater of metal sulphide mine at arid territory (BS mine, Western Australia). Trans Nonferrous Metals Soc China 20(8):1488–1493

Li RW (2011) Characteristics and control factors of ground water of Gejiu orefield. Yunnan Geol 1(30):64–66 (in Chinese)

Liu P, Hoth N, Drebenstedt C, Sun Y, Xu Z (2017) Hydro-geochemical paths of multi-layer groundwater system in coal mining regions - using multivariate statistics and geochemical modeling approaches. Sci Total Environ 601-602:1–14

Lu JZ (1985) Groundwater resources and the prospects of exploitation and utilization in Gejiu mining area. Site Investig Sci Technol 4:39–42 (in Chinese)

Nakhaei M, Amiri V, Rezaei K, Moosaei F (2015) An investigation of the potential environmental contamination from the leachate of the Rasht waste disposal site in Iran. Bull Eng Geol Environ 74(1): 233–246

Nejeschlebová L, Sracek O, Mihaljevič M, Ettler V, Kříbek B, Knésl I, Vaněk A, Penížek V (2015) Geochemistry and potential environmental impact of the mine tailings at Rosh Pinah, southern Namibia. J Afr Earth Sci 105:17–28

Ni CZ (2005) Research on the basalt and mineralization in Gejiu tin mine. Master's thesis, Kunming University of Science and Technology (in Chinese)

Nieto JM, Sarmiento AM, Olías M, Canovas CR, Riba I, Kalman J, Angel Delvalls T (2007) Acid mine drainage pollution in the Tinto and Odiel rivers (Iberian Pyrite Belt, SW Spain) and bioavailability of the transported metals to the Huelva estuary. Environ Int 33(4): 445–455

Pan HJ, Cheng ZZ, Yang R, Zhou GH (2015) Geochemical survey and assessment of tailings of the Gejiu tin-polymetallic mining area, Yunnan Province. Geol Chin 42(4):1137–1150

Pazand K, Javanshir AR (2014) Geochemistry and water quality assessment of groundwater around Mohammad Abad area, bam district, SE Iran. Water Qual Expo Health 6(4):225–231

Pazand K, Hezarkhani A (2012) Investigation of hydrochemical characteristics of groundwater in the Bukan basin, northwest of Iran. Appl Water Sci 2(4):309–315

Peng BJ, Li ST (2014) The present hydrogeology and protection, utilization of underground water in Gejiu orefield. Yunnan Geol 4(33): 594–600 (in Chinese)

Prasanth SVS, Magesh NS, Jitheshlal KV, Chandrasekar N, Gangadhar K (2012) Evaluation of groundwater quality and its suitability for

drinking and agricultural use in the coastal stretch of Alappuzha District, Kerala, India. Appl Water Sci 2(3):165–175

Pu T, He Y, Zhang T, Wu JK, Zhu GF, Chang L (2013) Isotopic and geochemical evolution of ground and river waters in a karst dominated geological setting: a case study from Lijiang basin, South-Asia monsoon region. Appl Geochem 33:199–212

Quispe D, Pérez-López R, Acero P, Ayora C, Nieto JM (2013) The role of mineralogy on element mobility in two sulphide mine tailings from the Iberian Pyrite Belt (SW Spain). Chem Geol 345(345):119–129

Sahoo PK, Tripathy S, Panigrahi MK, Equeenuddin SM (2016) Anthropogenic contamination and risk assessment of heavy metals in stream sediments influenced by acid mine drainage from a northeast coalfield, India. Bull Eng Geol Environ 76:537–552

Sánchez ERS, Hoyos SEG, Esteller MV, Morales MM, Astudillo AO (2017) Hydrogeochemistry and water-rock interactions in the urban area of Puebla Valley aquifer (Mexico). J Geochem Explor 181: 219–235

Sharma, SK (2008) Influence of sea water ingress: a case study from east coast aquifer in India. 20th salt water intrusion meeting:250–253

Smuda J, Dold B, Spangenberg JE, Friese K, Kobek MR, Bustos CA, Pfeifer HR (2014) Element cycling during the transition from alkaline to acidic environment in an active porphyry copper tailings impoundment, Chuquicamata, Chile. J Geochem Explor 140(3): 23–40

Sözen S, Orhon D, Dinçer H, Atesok G, Bastürkcü H, Yalcin T, Öznesil H, Karaca C, Alli B, Dulkadiroğlu H, Yağci N (2017) Resource recovery as a sustainable perspective for the remediation of mining wastes: rehabilitation of the CMC mining waste site in northern Cyprus. Bull Eng Geol Environ 76:1535–1547

Sun J, Tang C, Wu P, Strosnider WHJ, Han Z (2013) Hydrogeochemical characteristics of streams with and without acid mine drainage impacts: a paired catchment study in karst geology, SW China. J Hydrol 504(22):115–124

Triantafyllidis S, Skarpelis N, Komnitsas K (2007) Environmental characterization and geochemistry of Kirki, Thrace, NE Greece, abandoned flotation tailing dumps. Environ Forensic 8(4):351–359

Uddin MK (2017) A review on the adsorption of heavy metals by clay minerals, with special focus on the past decade. Chem Eng J 308: 438–462

Wang L, Ji B, Hu YH, Liu RQ, Sun W (2017) A review on in situ phytoremediation of mine tailings. Chemosphere 184:594–600

Wang XY, Shi ZM, Shi Y, Ni SJ, Wang RL, Xu W, Xu JY (2018) Distribution of potentially toxic elements in sediment of the Anning River near the REE and V-Ti magnetite mines in the Panxi rift, SW China. J Geochem Explor 184:110–118

Wickland BE, Wilson GW (2005) Self-weight consolidation of mixtures of mine waste rock and tailings. Can Geotech J 42(2):327–339

Ye M, Yan P, Sun S, Han D, Xiao X, Zheng L, Huang S, Chen Y, Zhuang S (2016) Bioleaching combined brine leaching of heavy metals from lead-zinc mine tailings: transformations during the leaching process. Chemosphere 168:1115–1125

Zhang LK, Qin XQ, Tang JS, Liu W, Yang H (2017) Review of arsenic geochemical characteristics and its significance on arsenic pollution studies in karst groundwater, Southwest China. Appl Geochem 77: 80–88

Zhao S (2014) Discussion of Mineral Processing Technology for High Tin High copper Symbiotic Sulphhide Ore in Gejiu. Multipurp Util Miner Resour 4:68–72 (in Chinese)

Zheng GQ, Fang XJ, Zhang HJ, Wang W (2009) Heavy metal pollution and vegetation restoration in Gejiu tin deposit in Yunnan province. Bull Soil Water Conserv 29(6):208–212

Zhuang YQ, Wang RZ, Yin JM (1996) Geology of the Gejiu tin-copper polymetallic deposit. Seismol Press (in Chinese)